PCCP

Concentration-dependent Luminescence of Ionic Liquids Consisting of Trialkyl(pentafluorocyclotriphosphazenyl)ammonium Moiety

Journal:	*Physical Chemistry Chemical Physics*
Manuscript ID:	CP-ART-07-2014-003181.R1
Article Type:	Paper
Date Submitted by the Author:	23-Aug-2014
Complete List of Authors:	Shiragami, Tsutomu; University of Miyazaki, Department of Applied Chemistry, Faculty of Engineering Nakamura, Yoko; University of Miyazaki, Matsumoto, Jin; University of Miyazaki, Otsuki, Masashi; Bridgestone Corporation, Yasuda, Masahide; University of Miyazaki, Department of Applied Chemistry, Faculty of Engineering

Concentration-dependent Luminescence of Ionic Liquids Consisting of Trialkyl(pentafluorocyclotriphosphazenyl)ammonium Moiety

Tsutomu Shiragami[*1], Yoko Nakamura[1], Jin Matsumoto[1], Masashi Otsuki[2], and Masahide Yasuda[1]

[1]Department of Applied Chemistry, Faculty of Engineering, University of Miyazaki, Gakuen-Kibanadai, Miyazaki 889-2192, Japan

[2]Central Reseach, Bridgestone Corporation, Ogawahigashi-Cho, Kodaira, Tokyo 187-8531, Japan

Corresponding author: Tsutomu Shiragami

Tel.: + 81 985 58 7313; fax: + 81 985 58 7315

E-mail address: t0g109u@cc.miyazaki-u.ac.jp

Abstract

Room-temperature ionic liquid compounds ($CpzNR_3^+X^-$) which were consisted of trialkyl(pentafluorocyclotriphosphazenyl)ammonium ($CpzNR_3^+$) and anion (X^-) such as chloride and bis(trifluoromethylsulfonyl)imide ($TFSI^-$) emitted blue luminescence under excitation of 360 nm. The luminescent quantum yields (Φ_{em}) of $CpzNR_3^+X^-$ were determined to be 0.012 – 0.044 in methanol solution at 360 nm excitation. The measurements of excitation spectra and luminescent lifetime (τ) indicated the existence of two luminescent species. The appearance of luminescence from pentafluorocyclotriphosphazenyl (Cpz) chromophore at longer wavelength and the dependence of luminescent intensity upon the concentration of $CpzNR_3^+X^-$ revealed that the observed luminescence should be attributed to *J*-aggregates of Cpz chromophore. The formation of their aggregates was also supported by concentration-dependence of chemical shift of ^{1}H-NMR. The *J*-aggregates involved both luminescent aggregates of smaller size with a shorter τ (1.0 ns) and those of the larger size with a longer τ (5.0 ns). It was observed that the Φ_{em} of aggregates with larger size was enhanced with the increase of concentration of $CpzNR_3^+X^-$. Thus, the luminescence stemming from luminescent aggregates can be explained reasonably by introducing "aggregation induced enhanced emission" (AIEE) mechanism.

Introduction

Room-temperature ionic liquids (RTILs) are well known to have unique properties such as a very small vapor pressure, high thermal stability, and ionic conductivity. Therefore, much attention has been paid to RTILs from viewpoint of solvent for synthesis and catalysis[1-2], extraction solvent,[3] and electrolyte materials.[4] Recently, a new property of luminescent RTILs are extending their application.[5-10] For example, Samanta, et al. have found that 1-methyl-3-butylimidazolium hexafluorophosphate ($BMIm^+PF_6^-$) had luminescence at visible light region, whose λ_{max} were depended on the excitation wavelength, although the luminescence from $BMIm^+$ itself were normally observed at UV region. They proposed that the aggregates of RTIL contributed to the luminescent mechanism.[5]

We have prepared nonflammable RTILs ($CpzNR_3^+X^-$) which were consisted of trialkyl(pentafluorocyclotriphosphazenyl)ammonium ($CpzNR_3^+$) and anion (X^-) such as chloride and bis(trifluoromethylsulfonyl)imide ($TFSI^-$): $CpzNR_3^+Cl^-$ (**1**) and $CpzNR_3^+TFSI^-$ (**2**) (Figure 1).[11] $CpzNR_3^+X^-$ showed unique properties such as non-dependence of viscosity on molecular weight and the large deviation from an ideal line in Walden plot. These suggested that $CpzNR_3^+X^-$ tends to form their aggregates easily.[12,13] Therefore, $CpzNR_3^+X^-$ may have a potential as a luminescent RTIL. Here, we report the luminescent properties of $CpzNR_3^+X^-$.

Figure 1.

Experimental

Instruments

UV-vis absorption and luminescent spectra of the solutions were obtained on a JASCO V-500 spectrophotometer and a Shimadzu RF-5300PC spectrophotometer, respectively. IR spectra were measured on a JASCO FT-IR 300. ^{1}H-NMR (400 MHz), ^{13}C-NMR (100 MHz), ^{31}P-NMR (162 MHz), and ^{19}F-NMR (376 MHz) spectra were taken in the $CDCl_3$ with a

Brucker AV 400M spectrometer. The tetramethylsilane was employed as an internal standard for the ^{1}H and ^{13}C NMR spectra. Moreover, triphenylphosphine oxide and trifluoroacetic acid were employed as internal standards in the ^{31}P and ^{19}F NMR measurements, respectively. Fast atom bombardment mass spectra (FAB-MS) were measured on a Hitachi M-2000AM in the positive ion mode.

Preparation of ionic liquids (1 and 2)

Pentafluorocyclotriphosphazenyl chloride (Cpz-Cl) was purchased from Bridgestone Corporation (Kodaira, Japan). Tertiary alkylamines (1.0 mmol) were added to Cpz-Cl (1.0 mmol) in diethyl ether (30 cm^3) and then the mixture were stirred for 1 h at 20 °C, resulting in $CpzNR_3^+Cl^-$ (**1**). After evaporating the solvent, **1** was subjected to an anion-exchange reaction by mixing a chloroform solution containing **1** (2.2 mmol) and lithium bis(trifluoromethylsulfonyl)imide (Li^+TFSI^-, 2.2 mmol, Aldrich). A light yellow liquid $CpzNR_3^+TFSI^-$ (**2**) was obtained after filtrating the precipitates of LiCl. The crude **2** was purified by centrifugal separation and active charcoal treatment. Similar treatment was applied to the purification of **1**.

In the ^{1}H-NMR spectra of $CpzNBu_3^+TFSI^-$ (**2b**), for example, the chemical shift (δ) of α-proton (H^a) of the butylamino group was shifted to a lower magnetic field (Δδ= 0.67 ppm) than that of the free butylamine, and the spin-spin coupling (J_{P-H} = 5.2 Hz) between the H^a and the P atom (P^N) bonded with an ammonium group was also observed. Furthermore, δ of P^N was shifted 23.5 ppm to higher magnetic field than that of the P-Cl in Cpz-Cl, showing clearly the transformation of the P-Cl bond to a P-N bond. Similar spectral data were obtained in other **1** and **2**. IR spectra of **1** and **2** revealed the characteristic absorption bands (957 cm^{-1} and 1279 cm^{-1}) due to the Cpz ring.[14] IR spectra of **2** gave two additional characteristic absorption bands due to $TFSI^-$; 1040 cm^{-1} (S=O) and 1200 cm^{-1} (C-F). In the ^{13}C-NMR, a

peak of CF_3 of $TFSI^-$ appeared at 119.56 ppm. From the intensity ratio of peaks between CF_3 and the carbon atom of the alkyl group in ^{13}C NMR spectra, the ion-exchange reaction from Cl^- to $TFSI^-$ proceeded quantitatively.

Butyldimethyl(pentafluorocyclotriphosphazenyl)ammonium chloride **(1a)**: ^1H NMR δ 0.96 (t, J= 7.3 Hz 3H), 1.40 (hex, J= 7.3 Hz, 2H), 1.71 (m, 2H), 2.69 (s, 6H), 2.84 (m, $J_{P\text{-}H}$= 5.3 Hz, 2H). ^{13}C NMR δ 13.4, 19.8, 26.8, 43.2, 56.0. ^{31}P NMR δ 3.2 (d, $J_{P\text{-}F}$= 873 Hz, t, $J_{P\text{-}P}$= 112 Hz, oct, $J_{P\text{-}F}$= 9 Hz, 1P), 10.6 (t, $J_{P\text{-}F}$= 899 Hz, 2P). ^{19}F NMR δ –72.7 (d, $J_{P\text{-}F}$= 899 Hz, 4F), –55.3 (d, $J_{P\text{-}F}$= 873 Hz, 1F).

Butyldimethyl(pentafluorocyclotriphosphazenyl)ammonium bis(trifluoromethylsulfonyl)imide **(2a)**: ^1H NMR δ 0.98 (t, J= 7.3 Hz 3H), 1.41 (hex, J= 7.3 Hz, 2H), 1.72 (m, 2H), 2.90 (s, 6H), 3.07 (m, $J_{P\text{-}H}$= 5.3 Hz, 2H). ^{13}C NMR δ 12.8, 19.1, 25.8, 42.4, 57.4, 119.3 (q, $J_{C\text{-}F}$= 321 Hz, $-CF_3$). ^{31}P NMR δ 3.1 (d, $J_{P\text{-}F}$= 873 Hz, t, $J_{P\text{-}P}$= 112 Hz, oct, $J_{P\text{-}F}$= 9 Hz, 1P), 10.6 (t, $J_{P\text{-}F}$= 899 Hz, 2P). ^{19}F NMR δ –73.0 (d, $J_{P\text{-}F}$= 899 Hz, 4F), –55.2 (d, $J_{P\text{-}F}$= 873 Hz, 1F), –82.6 (s, 1F, $-CF_3$). IR (neat): 920 cm^{-1} (ν_s P-N=P), 1040 cm^{-1} (ν S=O), 1200 cm^{-1} (ν C-F), 1355 and 1332 cm^{-1} (ν_{as} P-N=P). FAB-MS m/z = 332 (MH^+).

Tributyl(pentafluorocyclotriphosphazenyl)ammonium chloride **(1b)**: ^1H NMR δ 0.97 (t, J= 7.2 Hz 3H), 1.39 (hex, J= 7.2 Hz 2H), 1.72 (m, 2H), 2.93 (m, $J_{P\text{-}H}$= 5.2 Hz, 2H). ^{13}C NMR δ 13.1, 19.7, 25.3, 52.1. ^{31}P NMR δ 2.2 (d, $J_{P\text{-}F}$= 873 Hz, t, $J_{P\text{-}P}$= 107 Hz, oct, $J_{P\text{-}F}$= 10 Hz, 1P), 10.2 (t, $J_{P\text{-}F}$= 912 Hz, 2P). ^{19}F NMR δ –72.9 (d, $J_{P\text{-}F}$= 912 Hz, 4F), –55.1 (d, $J_{P\text{-}F}$= 873 Hz, 1F). IR (neat): 910 (ν_s P-N=P), 1292 and 1243 cm^{-1} (ν_{as} P-N=P).

Tributyl(pentafluorocyclotriphosphazenyl)ammonium bis(trifluoromethylsulfonyl)imide **(2b)**: ^1H NMR δ 0.97 (t, J= 7.2 Hz 3H), 1.40 (hex, J= 7.2 Hz 2H), 1.68 (m, 2H), 3.07 (m, $J_{P\text{-}H}$= 5.2 Hz, 2H). ^{13}C NMR δ 13.1, 19.5, 25.3, 52.0, 119.6 (q, $J_{C\text{-}F}$= 321.0 Hz, CF_3). ^{31}P

NMR δ 2.6 (d, $J_{P\text{-}F}$= 873 Hz, t, $J_{P\text{-}P}$= 111 Hz, oct, $J_{P\text{-}F}$= 9 Hz, 1P), 10.5 (t, $J_{P\text{-}F}$= 909 Hz, 2P). ^{19}F NMR δ –72.8 (d, $J_{P\text{-}F}$= 909 Hz, 4F), –54.7 (d, $J_{P\text{-}F}$= 873 Hz, 1F), –82.3 (s, 1F, CF_3). IR (neat): 924 (ν_s P-N=P), 1040 (ν S=O), 1197 (ν C-F), 1292 and 1243 cm^{-1} (ν_{as} P-N=P).

Hexyldimethyl(pentafluorocyclotriphosphazenyl)ammonium chloride **(1c)**: ^{1}H NMR δ 0.89 (t, J= 7.2 Hz 3H), 1.30 (m, 6H), 1.54 (m, 2H), 2.36 (s, 6H), 2.43 (m, $J_{P\text{-}H}$= 5.9 Hz, 2H). ^{13}C NMR δ 13.7, 22.3, 26.4, 26.7, 31.4, 44.6, 56.3. ^{31}P NMR δ 3.4 (d, $J_{P\text{-}F}$= 862 Hz, t, $J_{P\text{-}P}$= 118 Hz, oct, $J_{P\text{-}F}$= 9 Hz, 1P), 10.4 (t, $J_{P\text{-}F}$= 906 Hz, 2P). ^{19}F NMR δ –72.8 (d, $J_{P\text{-}F}$= 906 Hz, 4F), –55.5 (d, $J_{P\text{-}F}$= 862 Hz, 1F).

Hexyldimethyl(pentafluorocyclotriphosphazenyl)ammonium bis(trifluoromethyl-sulfonyl)imide **(2c)**: ^{1}H NMR δ 0.89 (t, J= 7.3 Hz 3H), 1.37 (m, 6H), 1.70 (m, 2H), 2.85 (s, 6H), 3.01 (m, $J_{P\text{-}H}$= 5.4 Hz, 2H). ^{13}C NMR δ 13.8, 22.3, 24.6, 26.1, 31.2, 43.2, 58.4, 119.8 (q, $J_{C\text{-}F}$= 320.9 Hz, –CF_3). ^{31}P NMR δ 3.5 (d, $J_{P\text{-}F}$= 830 Hz, t, $J_{P\text{-}P}$= 110 Hz, oct, $J_{P\text{-}F}$= 9 Hz, 1P), 11.4 (t, $J_{P\text{-}F}$= 882 Hz, 2P). ^{19}F NMR δ –72.6 (d, $J_{P\text{-}F}$= 882 Hz, 4F), –54.7 (d, $J_{P\text{-}F}$= 830 Hz, 1F), –82.3 (s, 1F, -CF_3). IR (neat): 920 (ν_s P-N=P), (S=O), 1200 (ν C-F), 1353 and 1332 cm^{-1} (ν_{as} P-N=P). FAB-MS m/z = 359 (MH^+).

Trioctyl(pentafluorocyclotriphosphazenyl)ammonium chloride **(1d)**: ^{1}H NMR δ 0.88 (t, J= 7.2 Hz 3H), 1.32 (m, 10H), 1.70 (m, 2H), 2.87 (m, 2H). ^{13}C NMR (100 MHz) δ 13.4, 22.0, 23.5, 26.3, 26.4, 28.5, 31.1, 52.3. ^{31}P NMR δ 2.1 (d, $J_{P\text{-}F}$= 874 Hz, t, $J_{P\text{-}P}$= 112 Hz, oct, $J_{P\text{-}F}$= 9 Hz, 1P), 10.2 (t, $J_{P\text{-}F}$= 921 Hz, 2P). ^{19}F NMR δ –73.0 (d, $J_{P\text{-}F}$= 921 Hz, 4F), –54.9 (d, $J_{P\text{-}F}$= 874 Hz, 1F). IR (neat): 915 (ν_s P-N=P), 1288 and 1246 cm^{-1} (ν_{as} P-N=P).

Trioctyl(pentafluorocyclotriphosphazenyl)ammonium bis(trifluoromethylsulfonyl)-imide **(2d)**: ^{1}H NMR δ 0.88 (t, J= 7.2 Hz 3H), 1.31 (m, 10H), 1.68 (m, 2H), 3.05 (m, $J_{P\text{-}H}$= 5.3 Hz, 2H). ^{13}C NMR δ 13.8, 22.4, 23.4, 26.3, 28.7, 28.8, 31.5, 53.3, 119.6 (q, $J_{C\text{-}F}$= 321.2 Hz, –CF_3). ^{31}P NMR δ 2.7 (d, $J_{P\text{-}F}$= 875 Hz, t, $J_{P\text{-}P}$= 111 Hz, oct, $J_{P\text{-}F}$= 9 Hz, 1P), 10.6 (t, $J_{P\text{-}F}$= 902

Hz, 2P). ^{19}F NMR δ –72.6 (d, $J_{P\text{-}F}$= 902 Hz, 4F), –54.6 (d, $J_{P\text{-}F}$= 875 Hz, 1F), –82.2 (s, 1F, -CF_3). IR (neat): 921 (ν_s P-N=P), 1040 (ν S=O), 1197 (ν C-F), 1352 and 1329 cm^{-1} (ν_{as} P-N=P).

Measurement of luminescent quantum yields and lifetimes

The luminescent spectra were measured in air-purged methanol solution at room temperature under excitation wavelengths at 360 nm and 440 nm. The quantum yields (Φ_{em}) for luminescence were determined using the following actinometers according to the reported method.[15] A methanol solution of 4-aminophathalimide (Tokyo Kasei), whose fluorescence quantum yield was 0.10, was used as an actinometer to determine Φ_{em} under the excitation at 360 nm.[5] As an actinometer under the excitation at 440 nm, methanol solution of 4,4-difluoro-1,3,5,7,8-pentamethyl-4-bora-3a,4a-diaza-S-indacene-2,6-disulfonic acid (BDPY) (Aldrich) was used. The fluorescence quantum yield of BDPY was 0.30. The luminescent lifetimes were measured on a Hamamatsu Photonics C4780 system based on a streak detector. An Nd^{3+} YAG laser (EKSPLA PL2210JE, 355 nm, FWHM 25 ps, 1 kHz) was used for excitation.

Results and Discussion

Preparation of 1 and 2 and their morphology at room-temperature

$CpzNR_3^+Cl^-$ (**1**) were prepared by the reaction of Cpz-Cl (1.0 mmol) with tertiary alkylamines (1.0 mmol) in diethyl ether (30 cm^3) for 1 h at 20 °C.[11] After the removal of the precipitates of LiCl from reaction mixture by filtrating, a light yellow liquid (cured **1**) was obtained. The **1** was purified by centrifugal separation and active charcoal treatment in order to remove the precipitate and colored materials. However, **1a** and **1c** were obtained as a white solid. The **1d** was like wax at 20 °C and became a brownish liquid over 40 °C. Thus

most of **1** did not show ionic liquid character except for **1b** which was brownish liquid at room temperature. Therefore, **1** was subjected to an anion-exchange of Cl^- to $TFSI^-$ by mixing a chloroform solution containing **1** (2.2 mmol) and Li^+TFSI^- (2.2 mmol) to give $CpzNR_3^+TFSI^-$ (**2**). The **2** was a pale colored liquid at room temperature (20 °C) (Table 1). The **1b** and **2** were soluble in ethyl acetate, chloroform, dichloromethane, acetone, acetonitrile, and methanol but insoluble in hexane. It was noteworthy that **1b** and **2** were insoluble in water despite they were ionic compound.

Table 1

Luminescent properties of ionic liquids

Cpz-Cl showed an absorption peak with absorption maximum at 262 nm in methanol and sharp fluorescence peak with maximum luminescent wavelength (λ_{max}) at 283 nm under excitation at 262 nm (Figure 1). However, under excitation at longer wave length at 360 nm and 440 nm, no luminescence appeared from the Cpz-Cl. On the other hand, RTILs such as **1b** and **2** showed the blue luminescence in the methanol solution and neat liquid under irradiation at 360 nm. An example was shown in Figure 2 where a broad luminescence from methanol solution containing **2a** (0.1 M) observed at 440 nm under the irradiation at 360 nm. We can watch the luminescence clearly even with eyes under irradiation of black light. Also, similar luminescence was observed from **2a** at 496 nm under excitation at 440 nm. The λ_{max} and luminescent quantum yield (Φ_{em}) of **2** are summarized in Table 3. The values of Φ_{em} (0.012 – 0.044) at 360 nm-excitation were much larger compared with that (0.005) of $BMIm^+PF_6^-$ reported by Samanta, et al.[5] On the other hand, no luminescence was observed in the case of **1a** with same $CpzN(Bu)Me_2^+$ cation part as **2a** (Table 1). Thus, the characteristic luminescence were observed under only state of RTILs.

In order to examine the luminescent species, the excitation spectra of **2** were measured

in methanol solution (Figure 3). For example, in two excitation spectra of **2c** monitored at 466 nm and 486 nm, almost same peak were observed at λ_{max} = 376 nm. Furthermore, the excitation spectrum monitored at 544 nm was measured, resulting in the peaks at λ_{max} = 378 nm and 527 nm which were different shape from the excitation spectra at 466 nm. Two luminescence of **2c** at 378 nm and 527 nm had the different lifetimes (τ) which were determined to be 1.0 ns and 5.0 ns, respectively. Accordingly, it is strongly indicated that two kinds of luminescent species should exist in **2c** solution.

Figures 1, 2 and 3 and Table 3

Concentration-dependent luminescence of RTILs

As described above, the λ_{max} of luminescence of **2** was different from that of Cpz-Cl. Moreover, the **2a** has broad absorptions around 450 nm which was apparently different from that of Cpz-Cl and non-RTIL **1a** whose absorptions were shifted to the shorter wavelength than that of **2a** (Figure 4). These results also support the existence of aggregates of **2** in methanol solution. It was speculated that aggregation may be *J*-aggregates type.[16]

Dependence of the luminescent spectra of **2** on their concentration was investigated in order to prove that the aggregates of **2** were the luminescent species at the longer wavelength. Figure 5 shows the luminescent spectra at various concentration of **2c** (0.01 M – 0.1 M) in methanol solution under the excitation at 360 nm. The λ_{max} of luminescence was shifted to the longer wavelength from 432 nm to 446 nm as the increase of concentration of **2c**. This result suggests that the luminescent species strongly should depend on the concentration of **2c.** Moreover, it is safely excluded that observed luminescence come from an impurity in **2c**.

The spectral changes were evaluated by relative fraction (%) of luminescent intensity at each wavelength for the sum (100%) of three luminescent intensities at 450 nm, 500 nm, and 550 nm. For example, in the case of **2c** whose concentration was 0.01 M, each luminescent

component at 450 nm, 500 nm, and 550 nm becomes 63%, 20%, and 8%, respectively (Figure 6). The fraction of luminescent component at longer wavelength (500 nm and 550 nm) tended to increase with the increase of concentration of **2c**. These phenomena can be interpreted by a change of distribution equilibrium of two luminescent aggregates with the dependence of a change of concentration of **2c**. Accordingly, it is suggested that a series of observed luminescence should be attributed to the formation of several kinds of *luminescent aggregates*,[5, 9, 10] in which the smaller size aggregates as an luminescent spices (τ = 1.0 ns) and the larger size aggregates as an luminescent spices (τ = 5.0 ns) were mainly included.

Figures 4, 5, and 6

Structure of aggregates and luminescent mechanism

The structure of aggregates was elucidated by the NMR spectra which were measured on the various concentration of **2c** (0.01 M – 1.0 M) in chloroform-*d*. Figure 7 shows the concentration dependence of the chemical shifts of H^a-H^e where $\Delta\delta$ denotes the differences ($\delta - \delta_{std}$) in chemical shifts between the peak (δ) at given concentration and standard peak (δ_{std}) at a concentration of 0.01 M. The chemical shifts of H^a and H^e were shifted with the increase of concentration of **2c**, whereas the chemical shifts of H^b, H^c, and H^d were almost constant even with the increase of concentration of **2c**. The chemical shifts of H^a and H^e shifted to the higher magnetic field and to the lower magnetic field, respectively. It indicated that the observed shifts can be attributed to the aggregates, not the change of polarity by high concentration of **2c** simply, because the shifts were observed for only specified proton.

Figure 7

The luminescence stemming from the aggregates of **2** may be phenomena owing to "aggregation induced enhanced emission (AIEE).[17, 18] The AIEE means that the emission

intensity of dye is enhanced by promoting the formation of dye aggregates by something methods, although the dye shows no emission under isolated state in solution. A reason why the emission intensity is enhanced is explained as due to regulating the emotion of chromophore by aggregation of dye. Recently it has been reported that AIEE was induced by the aggregation of chromophore as an anionic part of RTILs.[9] Therefore, our cases may be also regarded as AIEE induced by the aggregation of Cpz chromophore as a cationic part of RTILs. Figure 8 shows the dependence of concentration of **2c** upon Φ_{em}. The Φ_{em} obtained by 360 nm excitation was independent upon the changing concentration of **2c**, where the absorbance of **2c** at 360 nm was too large to determine Φ_{em} in the case of 1.0 M. On the other hand, the Φ_{em} obtained by 440 nm excitation increased with the increase of concentration of **2c**, implying the enhancement of luminescence can be induced due to the increase of rigidity of Cpz moiety in the larger size aggregates. The reason why Φ_{em} of **2d** is highest can be also explained as due to the increase of rigidity induced by stronger hydrophobic interaction among three long octyl chains. Accordingly, the present effect can be just explained as an AIEE.

A plausible structure of aggregates of **2** was shown in Scheme 2, based on the NMR date of Figure 8. Especially, our attention was paid to chemical shift of H^a because it shifted to the high magnetic field probably owing to the ring current of Cpz. Therefore, it can be inferred that H^a locates over another Cpz ring as the formation of aggregation. The shift of H^e, located in terminal of alkyl chain, to low magnetic field may also be due to the formation of aggregation. Furthermore, the observation of luminescence from Cpz at the longer wavelength than that from original Cpz (Figure 1) indicate that the luminescent aggregates of **2** should be *J* type of aggregates. So, a part of **2** in solution can take two kinds of *J*-aggregates having the structure of different size as shown in Scheme 2, although the aggregation number is unclear yet.

Figure 8 and Scheme 2

Conclusion

2 and **1b** are luminescent RTIL partly with two kinds of *J*-aggregates with a different size in methanol solution. Although the molar conductivity (Λ) values were not enough for utilizing as battery electrolytes,[11] **2** can be used as a unique luminescent material. Since the color of luminescence (λ_{max}) depends on the size of aggregates, it will be expected that **2** work as a color-tunable luminescent RTIL, if the size of aggregates could be controlled by hybridization of **2** with polymer matrixes or porous materials.

Acknowledgement

This work was partially supported by a Grant-in-Aid for Scientific Research (C) (No. 23550159) from the Japan Society for the Promotion of Science (JSPS). We thank Dr. Tetsuya Shimada (Tokyo Metropolitan University) and Prof. Haruo Inoue (Tokyo Metropolitan University) for the measurement of luminescent life time.

References

1 (a) P. Wasserscheid and T. Welton, *Ion Lquids in Synthesis*, Wiley-VCH, Weinheim Germany, 2003. (b) T. Itoh, E. Akasaki, K. Kubo and S. Shirakami, *Chem. Lett.*, 2001, 262–263.

2 J. P. Hallet and T. Welton, *Chem. Rev.*, 2011, **111**, 3508–3576.

3 J. G. Huddleston and R. D. Rogers, *Chem. Commun.* 1998, 1765–1766.

4 M. Yoshizawa, A. Narita and H. Ohno, *Aust. J. Chem.*,2004, **57**, 139–144.

5 (a) A. Paul, P. K. Mandel and A. Samanta, *Chem. Phys. Lett.*, 2005, **402**, 375–379. (b) A. Paul, P. K. Mandel and A. Samanta, *J. Phys. Chem. B*, 2005, **109**, 9148–9153.

6 Z. Chen, S. Zhang, X. Qi, S. Liu, Q. Zhang and Y. Deng, *J. Mater. Chem*., 2011, **21**, 8979-8982.

7 P. S. Campbell, M. Yang, D. Pitz, J. Cybinska and A. V. Mudring, *Chem. A. Eur. J.*, 2014, **20**, 4704–4712.

8 E. T. Spielberg, E. Edengeiser, B. Mallick, M. Havenith and A. V. Mudring, *Chem. A. Eur. J.*, 2014, **20**, 5338–5345.

9 (a) I. F. Pierole and I. E. Pacios, *J. Fluorescence* 2012, **22**, 145–150. (b) I. F. Pierole and Y. Agzenai, *J. Phys. Chem. B*, 2012, **116**, 3973–3981.

10 E. Binetti, A. Panniello, L. Triggiani, R. Tommasi, A. Agostiano, M. L. Curri and M. Striccoli, *J. Phys. Chem. B*, 2012, **116**, 3512–3518.

11 T. Shiragami, Y. Nakamura, J. Matsumoto, M. Otsuki and M. Yasuda, *Chem. Lett.*, 2010, **39**, 1006–1007.

12 (a) Y. Tsukuda, K. Iwamoto, H. Furutani, Y. Matsushita, Y. Abe, K. Matsumoto, K. Monda, S. Hayase, M. Kawatsuwa and T. Itoh, *Tetrahedron Lett*., 2006, **47**, 1801–1804. (b) M. Yoshino, R. J. Brodd and A. Kozawa, *Li-ion Batteries: Science and Technologies*, Springer Science+Business Media. New York, 2009, p. 275.

13 M. Yoshizawa, W. Xu and C. A. Angell, *J. Am. Chem. Soc.*, 2003, **125**, 15411–15419.

14 L. G. Lund, N. L. Paddock. J. E. Proctor and H. T. Searle, *J. Chem. Soc.,* 1960, 2542–2547.

15 J. B. Birks, *Photophysics of Aromatic Molecules*, Wiley/Interscience, New York, 1970 (Chapter 4).

16 F. Wurthner, T. E. Kaiser and C. R. Saha-Moller, *Angew. Chem. Int. Ed*., 2011, **50**, 3376–3410.

17 (a) S. Choi, J. Bouffard and Y. Kim, *Chem. Sci.*, 2014, **5**, 751–755. (b) Y. –Z. Xie, G. –G. Shan, P. Li, Z. –Y. Zhou and Z. –M. Su, *Dyes and Pigment*, 2013, **46**, 467–474.

18 (a) S. Kamio, Y. Hori, S. Komada, K. Minoura, H. Ichikawa, J. Horigome, A. Tatsumi, S. Kaji, T. Yamaguchi, Y. Usami, S. Hirota, S. Enomoto and Y. Fujita, *Chem. Commun*., 2010, **46**, 9013–9015. (b) W. Tang, Y. Xiay and A. Tong, *J. Org. Chem.*, 2009, **74**, 2163–2166.

Figure captions

Figure 1. Fluoresence spectra of Cpz-Cl (0.1 M) in methanol solution at 262 nm excitation.

Figure 2. Luminescent spectra of **1a** and **2a** in methanol solution under excitation at 360 nm (A) and 440 nm (B).

Figure 3. Excitation spectra were monitored at 466 nm (——), 486 nm (– · –) and 544 nm (– – –). The luminescent spectrum (– · · –) spectra of **2c** was measured in methanol solution under excitation at 360 nm Absorption (- - -) spectra of **2c** was measured in methanol solution.

Figure 4. Absorption spectra of **1a** and **2a** in methanol solution.

Figure 5. Luminescent spectra at various concentrations of **2c** (0.001 M – 0.1 M) in methanol solution under 360 nm excitation. The signals around 410 nm are Raman signal of solvent.

Figure 6. Ratio of luminesent intensity at each wavelength for the sum of three luminescent intensities at 450 nm (black bar), 500 nm (gray bar), and 550 nm (white bar) at various concentrations of **2c** (0.01 M – neat).

Figure 7. Plots of the differences ($\Delta\delta = \delta - \delta_{std}$) between chemical shifts (δ) measured at given concentration and those (δ_{std}) at a concentration of 0.01 M versus concentration in ^{1}H-NMR of **2c**: Ha (●), Hb (◆), Hc (△), Hd (□) and He (○).

Figure 8. Dependence of Φ_{em} upon the concentration of **2c** (0.25 M – 1.00 M) in luminescent spectra under excitation at 360 nm (●) and 440 nm (■).

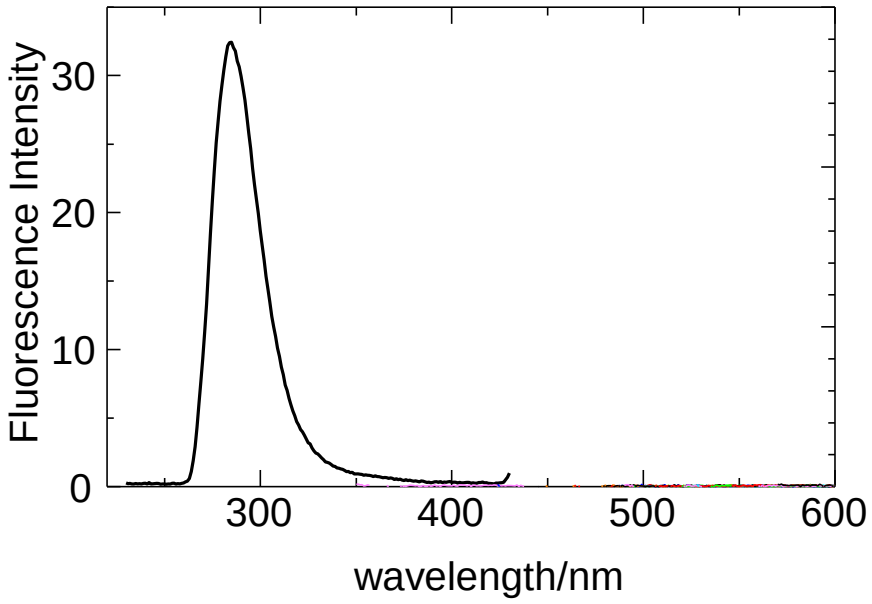

Figure 1. Fluoresence spectra of Cpz-Cl (0.1 M) in methanol solution at 262 nm excitation.

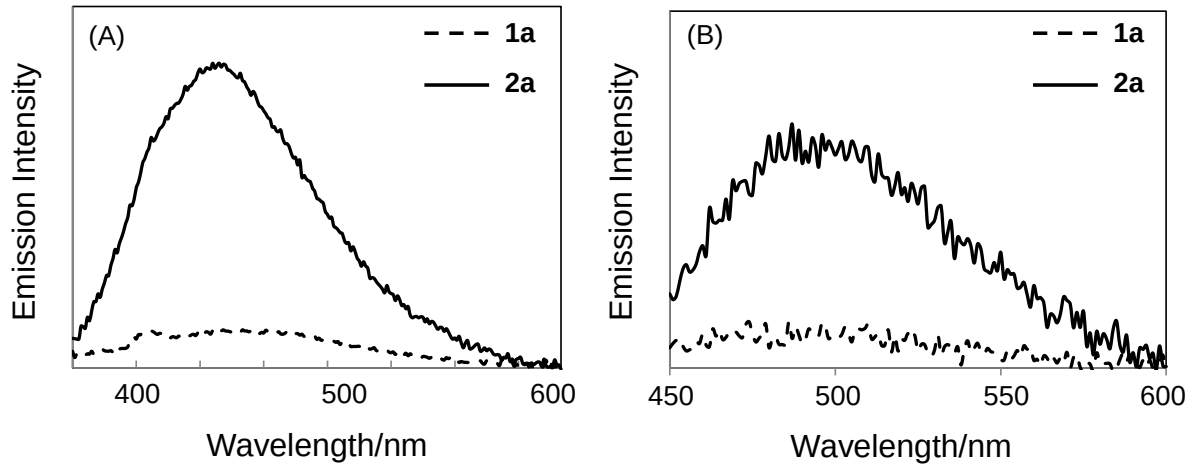

Figure 2. Luminescent spectra of **1a** and **2a** in methanol solution under excitation at 360 nm (A) and 440 nm (B).

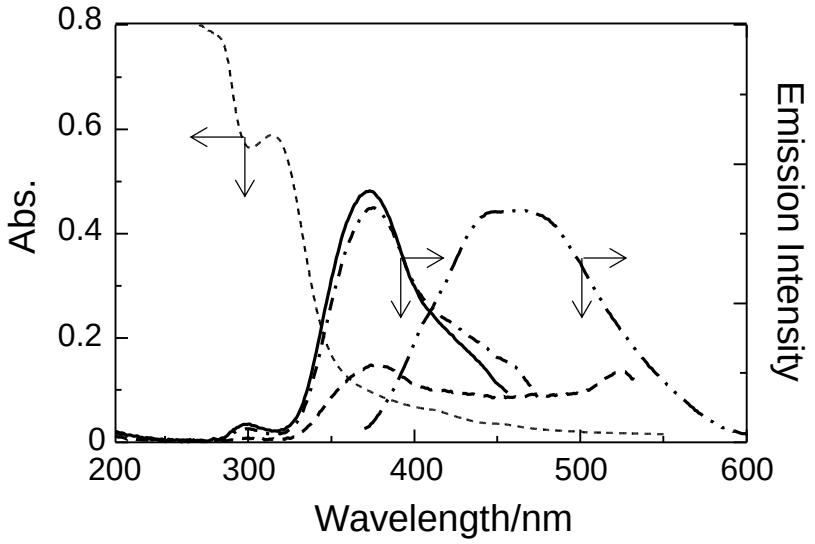

Figure 3. Excitation spectra were monitored at 466 nm (——), 486 nm (– · –) and 544 nm (– – –). The luminescent spectrum (– · · –) spectra of **2c** was measured in methanol solution under excitation at 360 nm. Absorption (- - -) spectra of **2c** was measured in methanol solution.

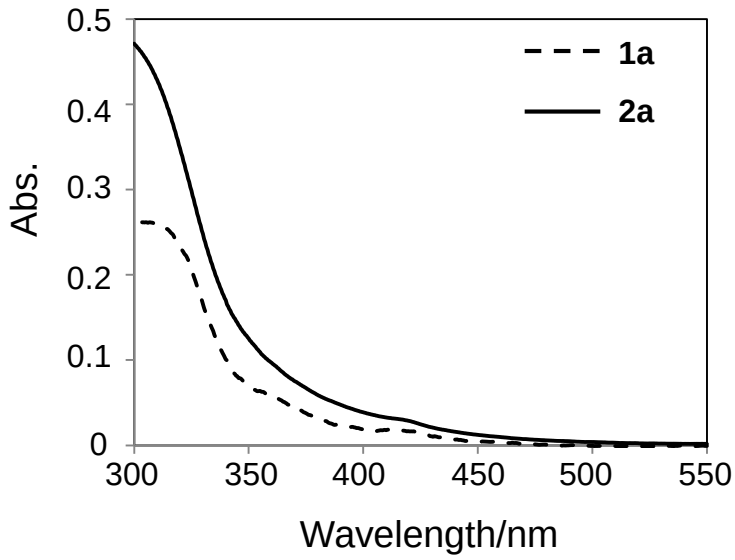

Figure 4. Absorption spectra of **1a** and **2a** in methanol solution.

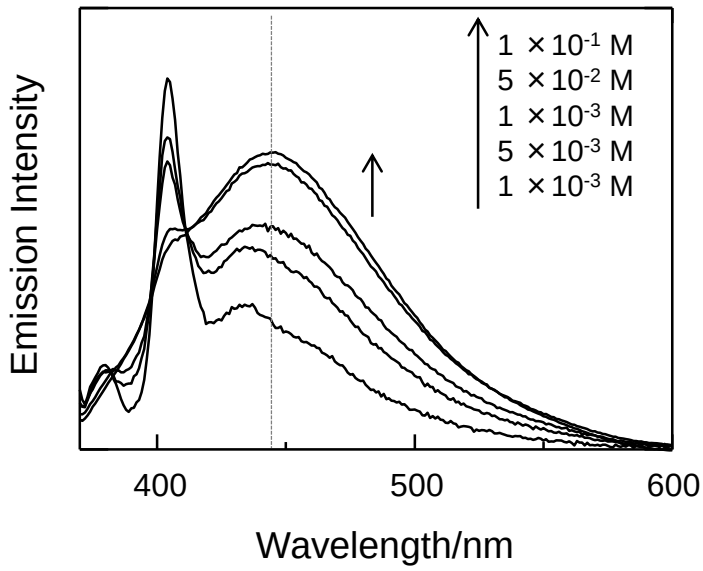

Figure 5. Luminescent spectra at various concentrations of **2c** (0.001 M – 0.1 M) in methanol solution under 360 nm excitation. The signals around 410 nm are Raman signal of solvent.

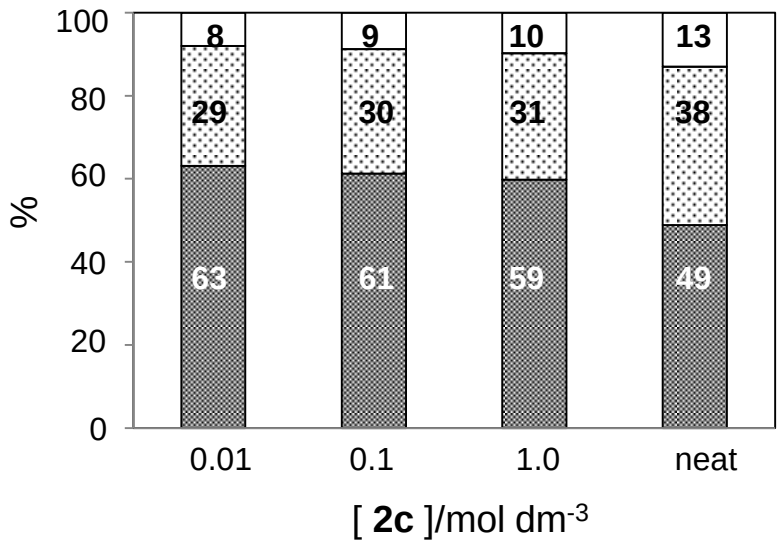

Figure 6. Ratio of luminesent intensity at each wavelength for the sum of three luminescent intensities at 450 nm (black bar), 500 nm (gray bar), and 550 nm (white bar) at various concentrations of **2c** (0.01 M – neat).

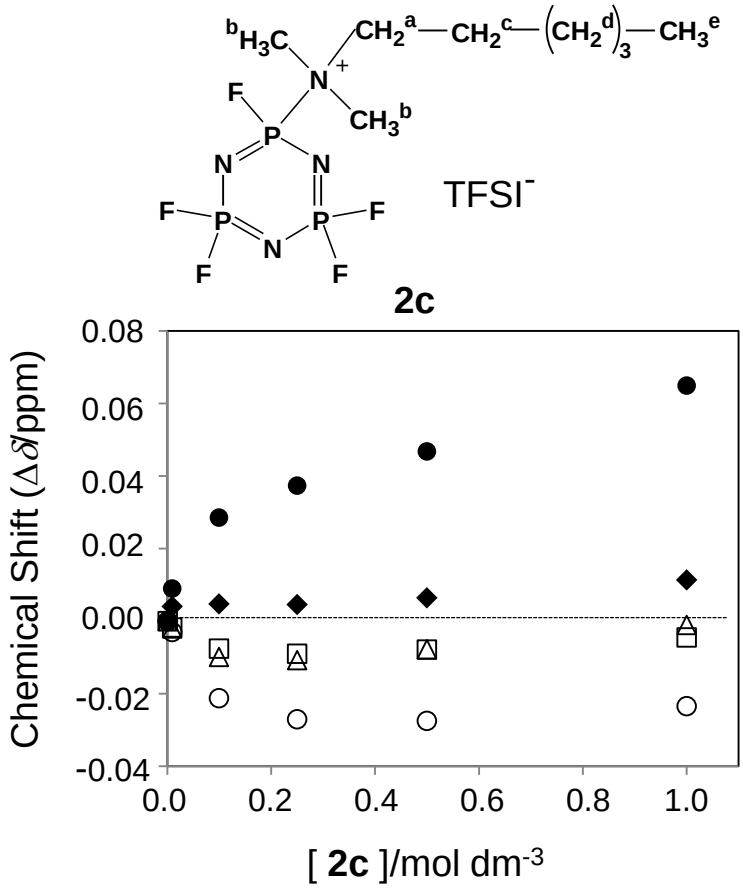

Figure 7. Plots of the differences ($\Delta\delta = \delta - \delta_{std}$) between chemical shifts (δ) measured at given concentration and those (δ_{std}) at a concentration of 0.01 M versus the concentration of **2c** in ^{1}H-NMR: Ha (●), Hb (◆), Hc (△), Hd (□) and He (○).

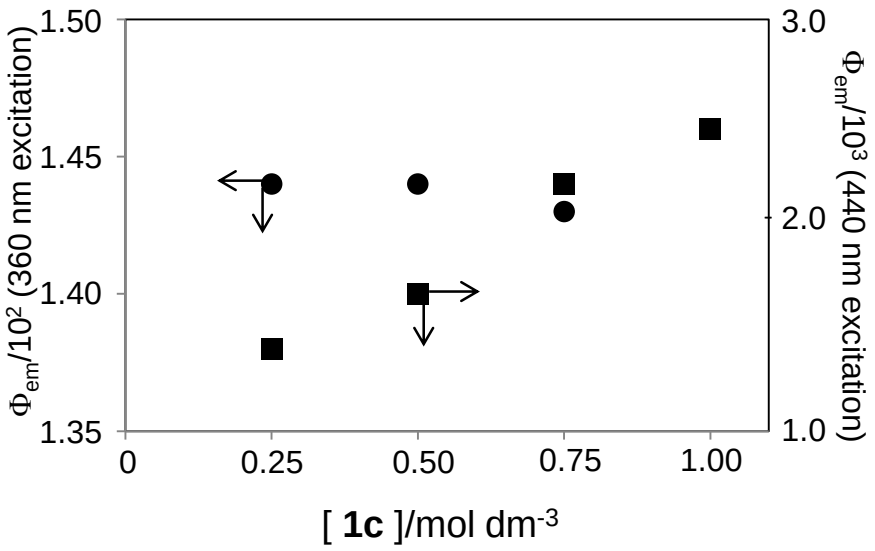

Figure 8. Dependence of Φ_{em} upon the concentration of **2c** (0.25 M – 1.00 M) in luminescent spectra under excitation at 360 nm (●) and 440 nm (■).

Table 1. Yields and State of $CpzNR_3^+X^-$

$CpzNR_3^+X^-$	Yield(%) [a]	State [b]	Color [c]
1a	35	S	W
1b	17	L	BT
1c	38	S	W
1d	13	W	Y
2a	16	L	W
2b	4	L	T
2c	5	L	YT
2d	13	L	BT

[a] Based on the starting material. [b] State at 20°C. L = liquid state, S = solid state. W = waxy [c] BT = brownish transparent, T = transparent, YT = yellowish transparent, W = white, Y = yellow.

Table 2. Maximum Luminescent Wavelength (λ_{max}) and Luminescent Quantum Yield (Φ_{em}) [a]

ILs	λ_{max}/nm [b]	λ_{max}/nm [c]	$\Phi_{em}/10^{2}$ [b]	$\Phi_{em}/10^{3}$ [c]
2a	440	496	1.2	7.2
2b	442	491	1.4	8.6
2c	445	504	1.4	2.3
2d	448	494	4.4	4.3

[a] The concentration of **2** are 1.0 M in methanol.

[b] Excited at 360 nm. [c] Excited at 440 nm.

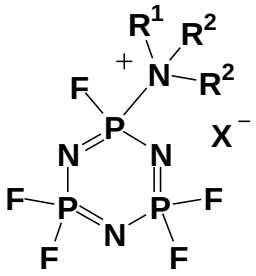

$R^1 = -(CH_2)_m-H$

$R^2 = -(CH_2)_n-H$

$TFSI^- =$ 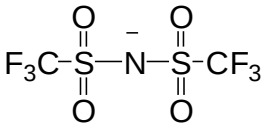

1a; *m* = 4, *n* = 1, X = Cl **2a**; *m* = 4, *n* = 1, X = TFSI

1b; *m* = *n* = 4, X = Cl **2b**; *m* = *n* = 4, X = TFSI

1c; *m* = 6, *n* = 1, X = Cl **2c**; *m* = 6, *n* = 1, X = TFSI

1d; *m* = *n* = 8, X = Cl **2d**; *m* = *n* = 8, X = TFSI

Scheme 1. Ionic liquids (**1** and **2)**.

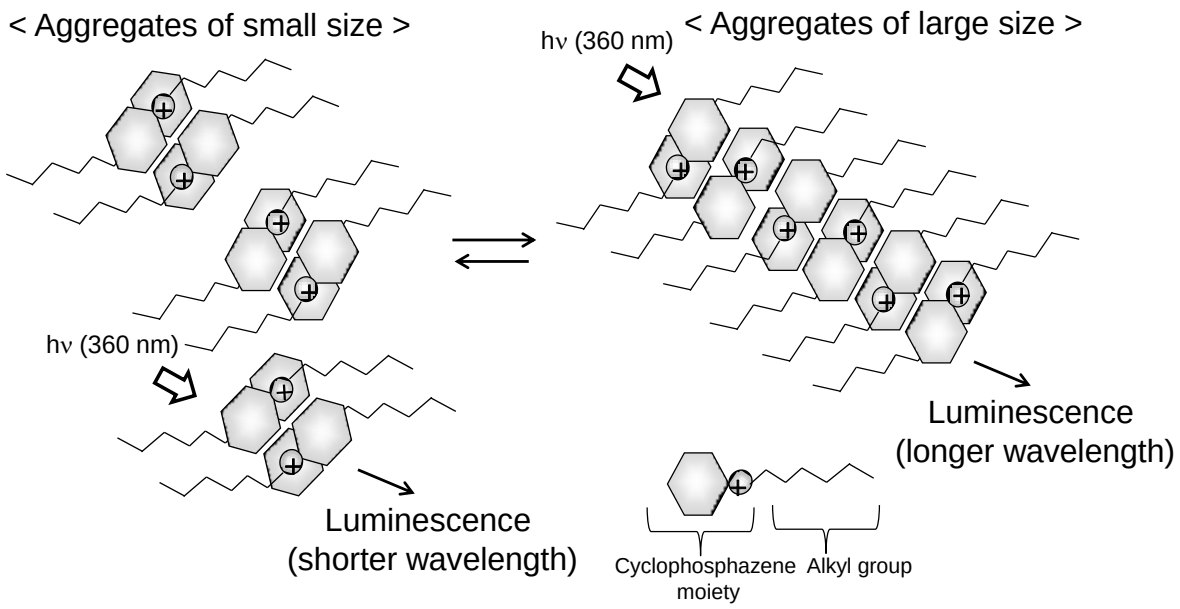

Scheme 2. Plausible structure of aggregates of **2**.